

Studies Pressure Drop of gas-Non-Newtonian Liquid Two Phase Flow in Bubble Column

Dr.Ali H. Jawad*

Received on:19/11/2008

Accepted on:22/1/2009

Abstract

An exclusive study has been done on experimental investigation of the two-phase flow pressure drop in an air-non-Newtonian liquid (CMC solutions) system in bubble column. The effects of gas and liquid flow rate on two-phase pressure drop have been illustrated. Experiments in a 0.2-m diameter, 2.4-m-high bubble column were carried out to determine the pressure drop. At the selected superficial velocities, two flow regimes were observed: heterogeneous bubbling flow and heterogeneous churn turbulent flow, they were identified through the slope changes in the plots of pressure drop and gas holdup. The pressure drop did not seem to be affected by the superficial liquid velocity and it was increased as the superficial gas velocity decreased or the CMC concentrations increased.

Keywords: Non-Newtonian fluids; Bubble columns; Hydrodynamics; Pressure drop

دراسة هبوط الضغط في نظام ثنائي الطور (غاز-سائل غير نيوتوني) في عمود فقاعي

الخلاصة

اعتمدت هذه الدراسة على التحقيق التجريبي من هبوط ضغط الطورين بالسائل الجوي غير النيوتوني (محلول CMC) نظام في عمود الفقاعة. تأثيرات الغاز ونسبة التدفق السائلة على هبوط ضغط المرحلتين صُوِّرَ. أما بالنسبة لجانب العملي تم استخدام عمود فقاعي قطره 0.2 م وبارتفاع 2.4 م لحساب الهبوط بالضغط. وبسرع مختلفة اخذنا نوعين من المسلك وهما (heterogeneous bubbling flow and heterogeneous churn turbulent flow) مَيَّزُوا خلال المنحدر يَتَغَيَّرُونَ مع هبوط الضغط وتعطيل الغاز. هبوط الضغط لم يَبْدُ لَكي يُؤَثِّرَ عليه بالسرعة السائلة السطحية وهو زادَ بينما سرعة الغاز السطحية قلت أو تراكيز CMC زادت.

Nomenclature

d	column diameter, (m).	P	Pressure drop , (N/m ²).
Fr _G	Froude number of the gas phase	Re _G	Reynolds number of the gas phase
(Fr _G = u ² gd)	characteristic length is the hydraulic radius of the bed.	(Re = $\frac{rud}{m}$)	in the case of non-
g	gravitational acceleration, (m/s ²).		Newtonian fluid (Re = $\frac{ru^{2-n}d^n}{k}$).
K	consistency index in the power-law model, (-).	u	axial velocity, (m/s).
n	flow index in the power-law model, (-)		

*Material Engineering Department, University of Technology/Baghdad

u_G superficial velocity of the gas phase (m/s).

u_L superficial velocity of the liquid phase (m/s).

Greek symbols

μ Newtonian viscosity (Kg/m.s).

Introduction

Bubble columns have been widely used as chemical reactors, and can be used to carry out various types of reactions. Among these, the following can be cited:

- Two-phase gas-liquid reactions: Most gas-liquid reactions use a homogeneous dissolved catalyst. Examples of these reactions are: partial oxidation of ethylene to acetaldehyde, isobutene separation from C4 cracking, production of dichloroethane.

- Three-phase, gas-liquid-solid reactions: Within these, there is a variety of operation modes (capacities, flow directions, moving or fixed). Some processes are: production of hydrogen peroxide, Fischer Tropsch synthesis, and biotechnological processes.

Another possible use of bubble columns is in the separation processes such as treatment

of various types of water (drinking, underground or wastewaters). Velázquez and Estévez (1992) demonstrated the potential that bubble columns have been used in the removal of trihalomethanes from drinking water and, by extension, of any volatile organic chemical (VOC). Also, bubble columns can be operated in different flow directions. The gas normally enters at the bottom, e.g., through a gas distributor. The liquid may be contained in the column (not flowing); this is often called semi batch or simply batch operation. The liquid may

ρ density at atmospheric conditions, (Kg/m³).

Subscripts

G gas phase.

L Liquid phase.

alternatively flow continuously at the bottom of the column, giving rise to a cocurrent or parallel flow operation. Less frequently, the liquid may flow downward and the operation is then called countercurrent. Even less frequently, the gas and the liquid are fed at the top of the column in a cocurrent downward flow operation. Liquid phase properties have been found to have an effect on the flow regime as it will be mentioned in next section. Additionally, the superficial velocities of the phases have also an effect on flow regimes. In bubble columns, aspect ratio (L/d) between 3 and 6 are recommended, although greater values have been used (Deckwer, 1992). Pressure drop is an important parameter from a design stand point since it not only affects the gas phase residence time but it also indirectly relates to the interfacial area. The knowledge of pressure drop also gives the pattern of energy dissipation, helps in modeling the system and forms the basis of assessment of performance of the equipment. Wang et al. (2004) present data on the interfacial friction factor and relative interfacial roughness on the gas-liquid interface for an air-water annular flow in a tube. Motil et al. (2003) report experimental data on flow regime transitions, pressure drop, and flow characteristics for co-current gas-liquid flow through packed columns in microgravity. Earlier, Bousman et al. (1996) presented data on twophase gas-liquid flow in the reduced gravity aircraft

for void fraction, liquid film thickness and pressure drop. Takamasa et al. (2003) present data which they claim can be used for the development of reliable constitutive relations which reflect the true transfer mechanisms in two-phase flow in microgravity.

These relations can be used to determine the pressure drop across the pipe section. Kamp et al. (2001) developed a mechanistic model for bubble coalescence in turbulent flow. Their model can be used to predict pressure drop in pipes. Iguchi and Terauchi (2001) reported wettability of the pipe did not affect the mean rising velocity of bubbles in microgravity. Taitel and Witte (1996) present a model to predict slug flow in microgravity.

Colin and Fabre (1995) reported how coalescence and the wall friction factor affect pressure drop. Mandal et al. (2004) reported the frictional pressure drop in downflow bubble column without considering the bubble-liquid interaction. The detailed literature survey regarding the pressure drop has been cited in our earlier study (Majumder et al., 2006a). From the literature review, it is seen that correlations based on experiments exist for predicting the pressure drop, but none of these approaches have taken into account the contacting mechanism between the phases, effect of bubble formation, phase interaction due to interaction of bubbles and the wettability effect on pressure drop in downflow bubble column with non-Newtonian system. In our earlier study (Majumder et al., 2006a), prediction of pressure drop characteristics in the downflow bubble column with only air-water system has been reported. In the present study, the same model (Majumder et al., 2006a) for pressure drop with a refinement in the ejector induced downflow bubble column

with non-Newtonian liquids has been incorporated.

The model which is based on mechanical energy balance within the framework of dynamic interaction of the phases has been formulated. The model includes the effect of bubble formation, phase interaction at interface and the wettability effect of liquid on the pressure drop. The theoretical

model proposed in the present study appears to predict the pressure drop satisfactorily for gas-liquid dispersed flow in the cocurrent gas non-Newtonian liquid downflow bubble column.

Experimental

The experimental setup is shown in Figure (1). The main components are: a column made up by two cylindrical sections of Plexiglas of 0.20 m of inner diameter and an entrance cone, a self-metering pump, two plastic feed tanks, filter devices, a rotameter to measure the gas flow rate, and a pressure transducer connected to a data acquisition system.

The pressure drop measurements were plotted to study the effect of liquid and gas superficial velocities on this variable. Similar plots were done to obtain the effect of CMC concentrations. Due to the presence of two slopes in these plots, two flow regimes were identified confirming the visual observations.

Two types of experiments were carried out: continuous (the gas and liquid phases are fed continuously in the column from in the bottom of the column, flowing in this case in ascendant and cocurrent mode) and semicontinuous modes (the gas phase flow in ascendant mode while the liquid phase was charged to the column at the beginning of the operation). First the CMC solution was prepared in one of the feed tanks. Runs were carried out at various gas and liquid superficial

velocities and at various concentrations of CMC.

By opening the appropriate valves and turning on the pump, the column was filled with the liquid phase. Using the micrometering valve, the air flow was set to a desired value of a gas superficial velocity, for the pump at different positions of the axis that permits to change the flow rate of liquid in it. When the column reached steady state, a pulse of tracer (aqueous methylene blue solution) was injected at the lowest sampling port and the samples were drawn from the highest sampling port. The samples were taken from the top until the blue color of the injected tracer tone down totally (continuous tests) or becomes homogeneous in all bubble column (batch tests). In addition, the pressure drop was recorded continuously by means of the pressure transducer and the data acquisition system. Then, the inlet

valves of air and liquid were closed and the pump turned off. The final height of the liquid in the column was measured after phase disengagement.

The procedure for semicontinuous operation was similar except that bubble column was filled with liquid, the pump was turned off and the exit valve of the pump to bubble column closed.

Results and discussion

The pressure drop obtained for tap water at different liquid superficial velocities through the differential pressure transducer is shown in Figure (2). This plot shows no effect on the pressure drop of the superficial liquid velocity in the range studied.

Additionally, it is seen that pressure drop decreased as superficial gas velocity increased, and this observation could be explained through the reduction of the mixture viscosity (because of the increase

of gas holdup in the bubble column) that caused the reduction of the shear stress in its component r_z and so that the pressure drop decreased.

Figures (3) and (4) show similar plots, but for 0.20 and 0.40% by weight aqueous solutions of CMC.

In Figure (5) the comparison between CMC concentrations is presented in batch mode of liquid ($u_L=0$ m/s). In this figure it is observed that pressure drop increases as CMC concentration in the liquid phase does due to the increase in the viscosity of the solution. The effect it is undistinguished at low superficial gas velocity. The same trend was found in Figure (6) that corresponds to continuous mode ($u_L=0.0045$ m/s).

Two flow regimes were observed in the bubble column in all concentrations of CMC. Both were heterogeneous because the presence of different bubble sizes in the bubble column; but the movement inside of them were different establishing two heterogeneous regimes: heterogeneous bubbling flow (described by Ramachandran and Chaudri, 1983) and heterogeneous churn turbulent flow (found by Vatai and Tekic, 1989, Soham, 1982). Two pictures were taken to illustrate both regimes and they are shown in Figure (7).

Taking into account the effect of CMC concentration (in terms of the power-law parameters) and the superficial gas velocity on pressure drop, it is possible to propose expressions to predict the last parameter as a function of the formers in both flow regime and for Newtonian (tap water) and non-Newtonian solutions. These expressions are shown in Table (1), and Table (2) shows analogous expressions but as a function of dimensionless numbers. It is important to mention that regression coefficients of equivalent expressions from Tables (1)

and (2) were similar; for this reason, the next figures corresponds to the correlations calculated from the Table (2). Figure (8) shows the behavior of correlations (Equations 5 and 6) obtained for water in both flow regimes for batch runs compared to experimental data, while Figure (9) shows analogous plot but at $u_L = 0.0045$ m/s. It is observed that proposed correlations fits experimental data.

The parity plot shown in Figure (10) compares the pressure drop obtained from experimental data and by equations (5) and (6) in the case of tap water as used fluid.

The values calculated with the proposed correlations are inside the 2% of deviation bars respect to straight line of 45°, indicating that data were fit quite well through the proposed correlations.

Figures (11) and (12) show the experimental data obtained with 0.20 and 0.40% by weight CMC solutions respectively and the fit of the correlations proposed through equations (7) and (8). Again, the plots show a good fit with the correlations.

Figure (13) shows a parity plot that compares the pressure drop obtained from experimental data and by using equations (7) and (8) for CMC solutions. The values calculated with the proposed correlations are within $\pm 2\%$ of the straight line at 45°, indicating that the proposed correlations fit quite well the experimental data.

Conclusions

The pressure drop characteristics of two-phase gas-non-Newtonian liquid flow in system have been studied in the present work. Effects of concentrations of CMC solution, gas and liquid flow rate on two-phase pressure drop have been critically examined. The superficial liquid velocity did not affect the pressure drop in the

range of liquid velocities considered. Two flow regimes were found in the bubble column studied: heterogeneous bubbling flow and heterogeneous churn turbulent flow. Empirical correlations were proposed to calculate the pressure drop for Newtonian and non-Newtonian fluids for the two flow regimes.

Reference

- [1] Bousman, W.S., McQuillen, J.B., Witte, L.C., 1996. Gas-liquid flow patterns in microgravity: effects of tube diameter, liquid viscosity and surface tension. *International Journal of Multiphase Flow* 22 (6), 1035–1053.
- [2] Colin, C., Fabre, J., 1995. Gas-liquid pipe-flow under microgravity conditions—influence of tube diameter on flow patterns and pressure drops. *Microgravity sciences: results and analysis of recent spaceflights. Advances in Space Research* 16 (7), 137–142.
- [3] Deckwer, W.D. *Bubble Column Reactors*, John Wiley & Sons. New York. pp.533. (1992).
- [4] Iguchi, M., Terauchi, Y., 2001. Microgravity effects on the rising velocity of bubbles and slugs in vertical pipes of good and poor wettability. *International Journal of Multiphase Flow* 27 (2), 189–2198.
- [5] Kamp, A.M., Chesters, A.K., Colin, C., Fabre, J., 2001. Bubble coalescence in turbulent flows: a mechanistic model for turbulence-induced coalescence applied to microgravity bubbly pipe flow. *International Journal of Multiphase Flow* 27 (8), 1363–1396.
- [6] Majumder, S.K., Kundu, G., Mukherjee, D., 2006a. Prediction of pressure drop in a modified gas-liquid downflow bubble column. *Chemical Engineering Science* 61 (12), 4060–4070.

- [7] Mandal, A., Kundu, G., Mukherjee, D., 2004. Studies on frictional pressure drop of gas-non-Newtonian two-phase flow in a cocurrent downflow bubble column. *Chemical Engineering Science* 59 (18), 3807–3815.
- [8] Motil, B.J., Balakotaiah, V., Kamotani, Y., 2003. Gas–liquid two-phase flow through packed beds in microgravity. *A.I.Ch.E. Journal* 49, 557–565.
- [9] Taitel, Y., Witte, L., 1996. The role of surface tension in microgravity slug flow. *Chemical Engineering Science* 51 (5), 695–700.
- [10] Takamasa, T., Iguchi, T., Hazuku, T., Hibiki, T., Ishii, M., 2003. Interfacial area transport of bubbly flow under microgravity environment. *International Journal of Multiphase Flow* 29 (2), 291–304.
- [11] Velázquez, C. and Estévez, L.A., “Stripping of trihalomethanes from drinking water in a bubble-column aerator,” *AIChE J.*, 38 (2), 211-218 (1992).
- [12] Wang, Z.L, Gabriel, K.S., Manz, D.L., 2004. The influences of wave height on the interfacial friction in annular gas–liquid flow under normal and microgravity conditions. *International Journal of Multiphase Flow* 30 (10), 1193–1211.

Table (1) Correlations for pressure drop.

Fluid	Regime	Correlation
Newtonian	Heterogeneous bubbling flow regime ($1.04 \times 10^{-3} \leq u_G \text{ (m/s)} \leq 1.44 \times 10^{-2}$)	$\Delta P \text{ (Pa)} = 18323 u_G^{-0.014}$ ---(1)
	Heterogeneous churn turbulent flow regime ($3.07 \times 10^{-2} \leq u_G \text{ (m/s)} \leq 4.62 \times 10^{-2}$)	$\Delta P \text{ (Pa)} = 14230 u_G^{-0.077}$ ---(2)
Non-Newtonian	Heterogeneous bubbling flow regime ($1.04 \times 10^{-3} \leq u_G \text{ (m/s)} \leq 1.44 \times 10^{-2}$)	$\Delta P \text{ (Pa)} = 18943 u_G^{-0.014n} k^{0.0064n}$ ----- (3)
	Heterogeneous churn turbulent flow regime ($3.07 \times 10^{-2} \leq u_G \text{ (m/s)} \leq 4.62 \times 10^{-2}$)	$\Delta P \text{ (Pa)} = 15791 u_G^{-0.086n} k^{0.0027n}$ ----- -(4)

Table (2) Correlations for pressure drop as a function of dimensionless number .

Fluid	Regime	Correlation
Newtonian	Heterogeneous bubbling flow regime ($1.04 \times 10^{-3} \leq u_G \text{ (m/s)} \leq 1.44 \times 10^{-2}$)	$\Delta P \text{ (Pa)} = 20995 Re_G^{-0.014}$ ---(5)
	Heterogeneous churn turbulent flow regime ($3.07 \times 10^{-2} \leq u_G \text{ (m/s)} \leq 4.62 \times 10^{-2}$)	$\Delta P \text{ (Pa)} = 29529 Re_G^{-0.077}$ ---(6)
Non-Newtonian	Heterogeneous bubbling flow regime ($1.04 \times 10^{-3} \leq u_G \text{ (m/s)} \leq 1.44 \times 10^{-2}$)	$\Delta P \text{ (Pa)} = 18514 n^{-0.042} Re_G^{0.0028n} Fr_G^{0.010n}$ ----- (7)
	Heterogeneous churn turbulent flow regime ($3.07 \times 10^{-2} \leq u_G \text{ (m/s)} \leq 4.62 \times 10^{-2}$)	$\Delta P \text{ (Pa)} = 16108 n^{0.16} Re_G^{0.0398n} Fr_G^{0.037n}$ ----- (8)

*The Reynolds number in the case of non-Newtonian fluids was calculated follows the definition of this number for this kind of fluids.

* k and n are the rheological parameters of the power-law mode

Table (3) Correlations data pressure drop for CMC solutions..

Run	CMC concentration (% wt)	u_G (m/s)	u_l (m/s)	Consistency index $K(\text{Pa}\cdot\text{s}^n)$	Flow index $n, (-)$	ΔP (pa) Correlations
1	0.2	0.001036	0	0.0113	0.9442	20126.30
2	0.2	0.008297	0	0.0161	0.9111	19614.50
3	0.2	0.01446	0	0.0074	0.9746	19423.51
4	0.2	0.030795	0	0.0135	0.9309	18666.55
5	0.2	0.038494	0	0.0121	0.9364	18296.78
6	0.2	0.046193	0	0.0107	0.9469	17989.41
7	0.2	0.001036	0.004509	0.0181	0.9063	20132.60
8	0.2	0.008297	0.004509	0.0110	0.9413	19591.95
9	0.2	0.01446	0.004509	0.014	0.9338	19477.60
10	0.2	0.030795	0.004509	0.0212	0.9025	18799.11
11	0.2	0.038494	0.004509	0.0107	0.9525	18267.20
12	0.2	0.046193	0.004509	0.0173	0.9059	18136.85
13	0.4	0.001036	0	0.1678	0.7284	20101.77
14	0.4	0.008297	0	0.0773	0.8150	19703.93
15	0.4	0.01446	0	0.0928	0.7952	19585.77
16	0.4	0.030795	0	0.0421	0.8537	18941.18
17	0.4	0.038494	0	0.0651	0.8339	18743.95
18	0.4	0.046193	0	0.0553	0.8446	18468.82
19	0.4	0.001036	0.004509	0.1529	0.7530	20133.13
20	0.4	0.008297	0.004509	0.2462	0.7008	19697.87
21	0.4	0.01446	0.004509	0.0991	0.7894	19587.53
22	0.4	0.030795	0.004509	0.0941	0.7956	19036.53

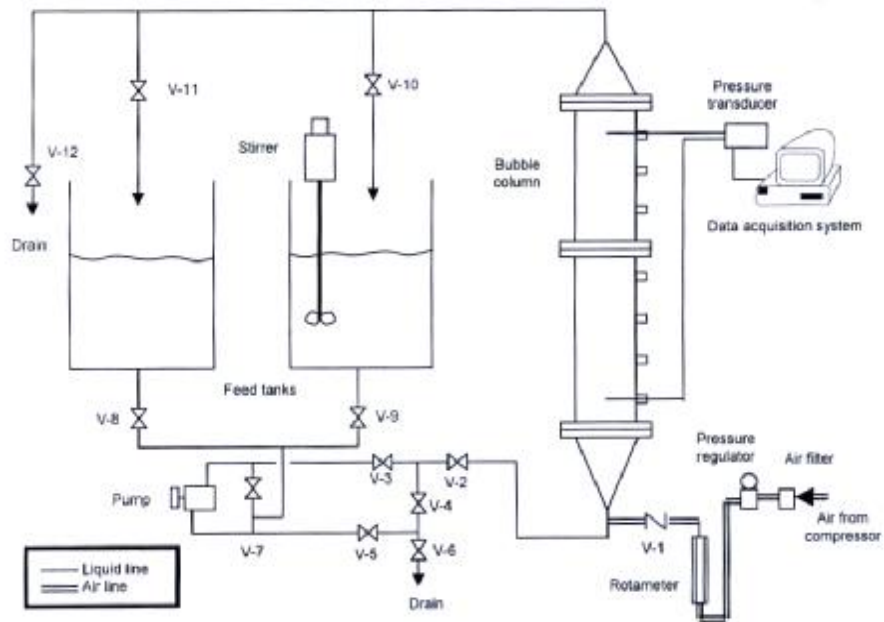


Figure (1) Experimental setup

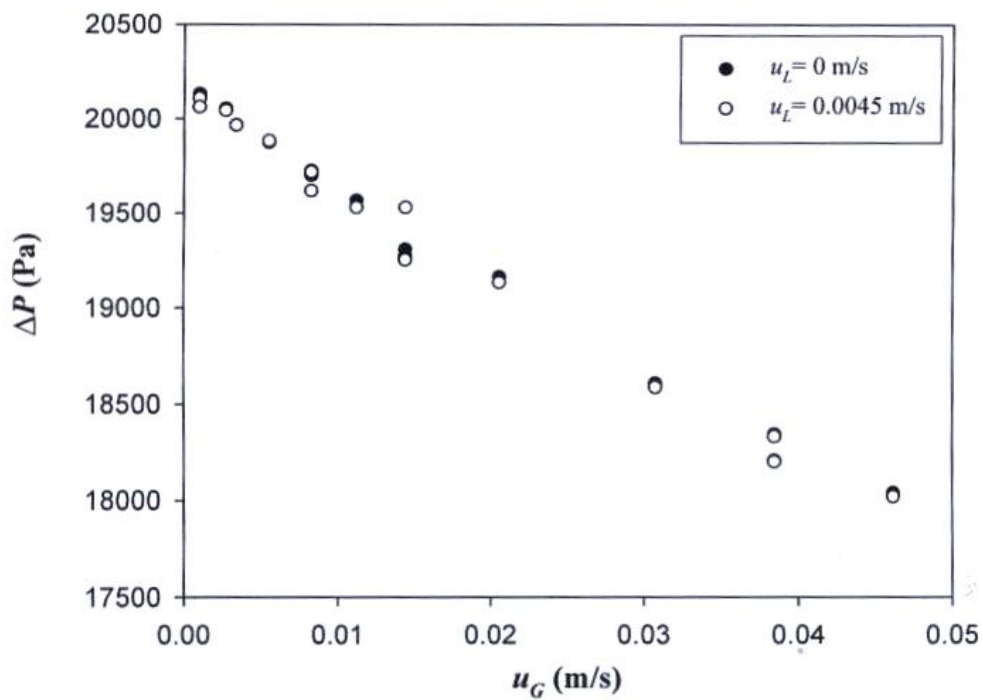


Figure (2) Pressure drop for tap water at different superficial velocities.

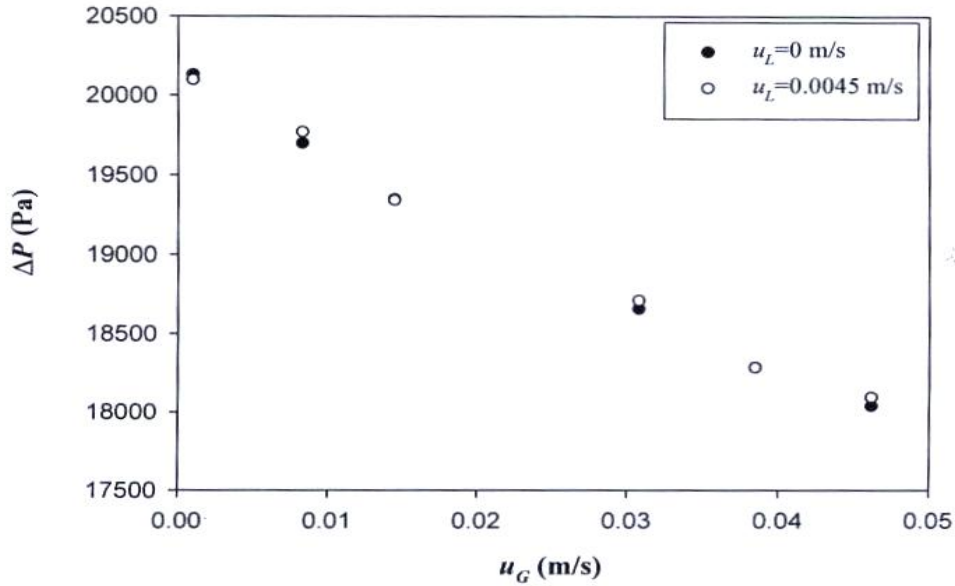


Figure (3) Pressure drop for 0.2% of CMC in water at different liquid superficial velocities.

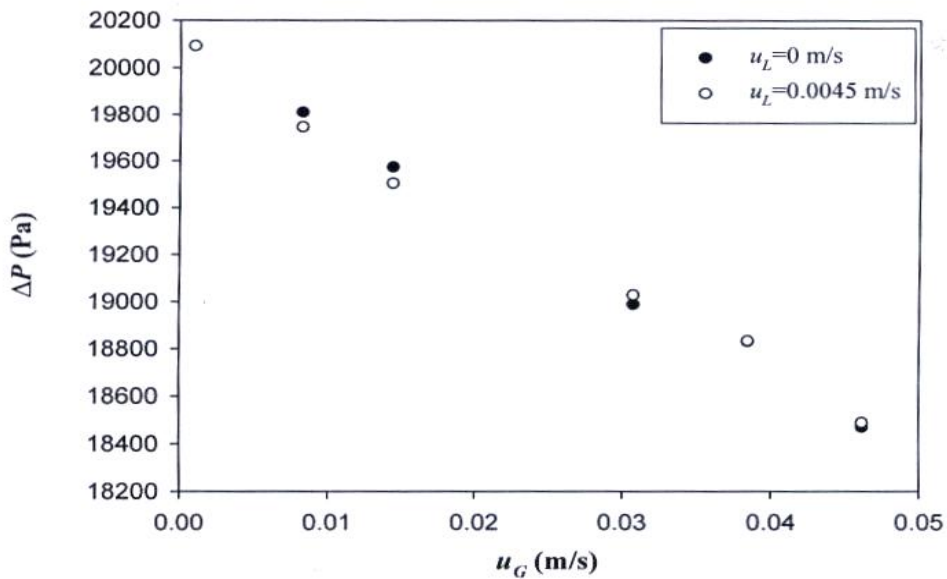


Figure (4) Pressure drop for 0.4% of CMC in water at different liquid superficial velocities.

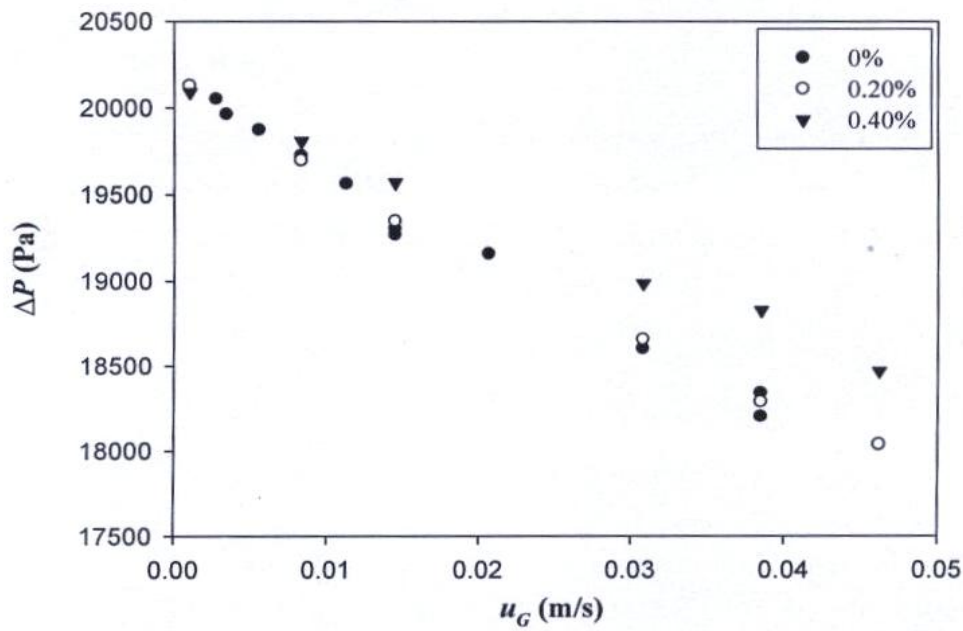


Figure (5) Pressure drop in batch mode at different CMC concentrations,.

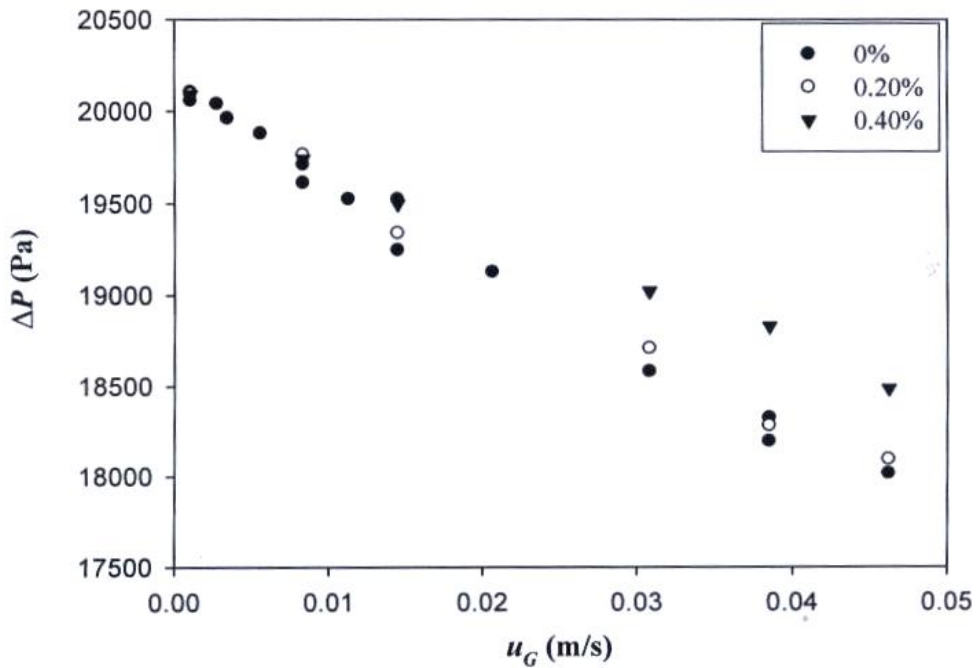


Figure (6) Pressure drop in continuous mode ($u_l=0.0045$ m/s) at different CMC concentrations,



a) Heterogeneous bubbling flow



(b) Heterogeneous churn turbulent

Figure (7): Flow regimes found in the range of the operation of the bubble column.

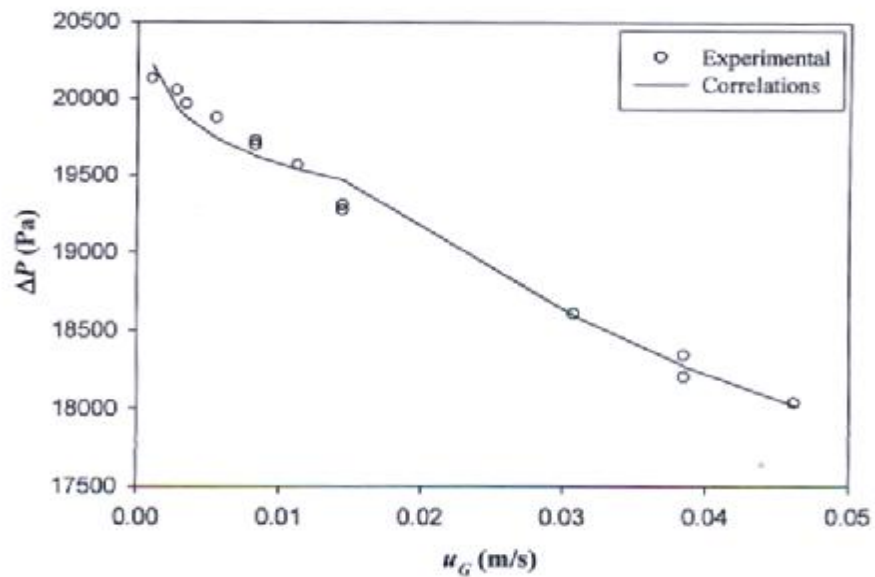


Figure (8): Pressure drop for tap water and $u_l=0\text{m/s}$.

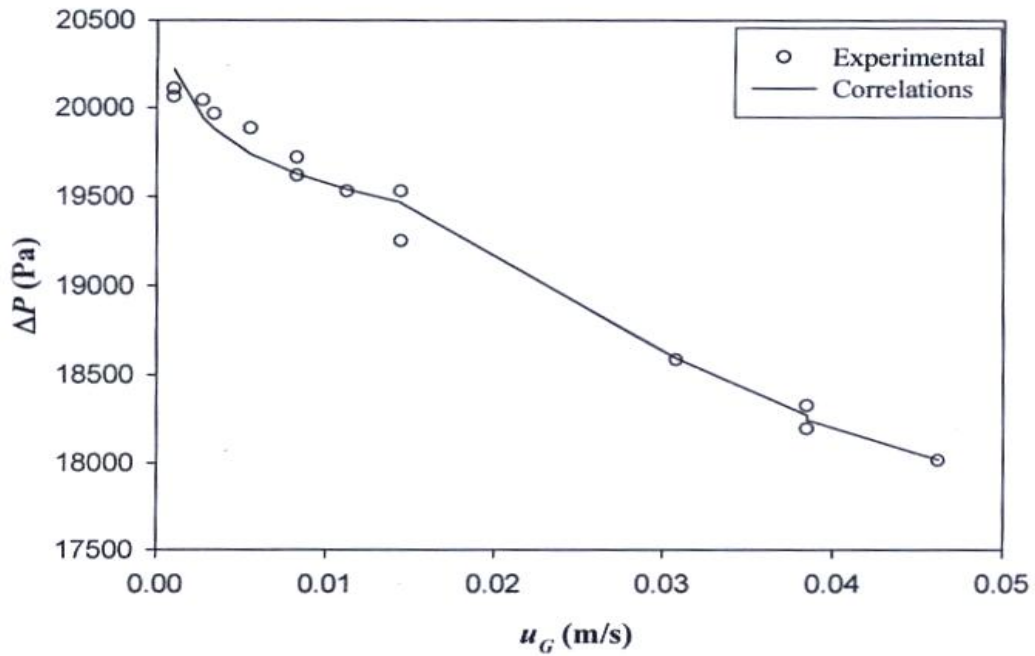


Figure (9): Pressure drop for tap water and $u_l=0.0045\text{m/s}$.

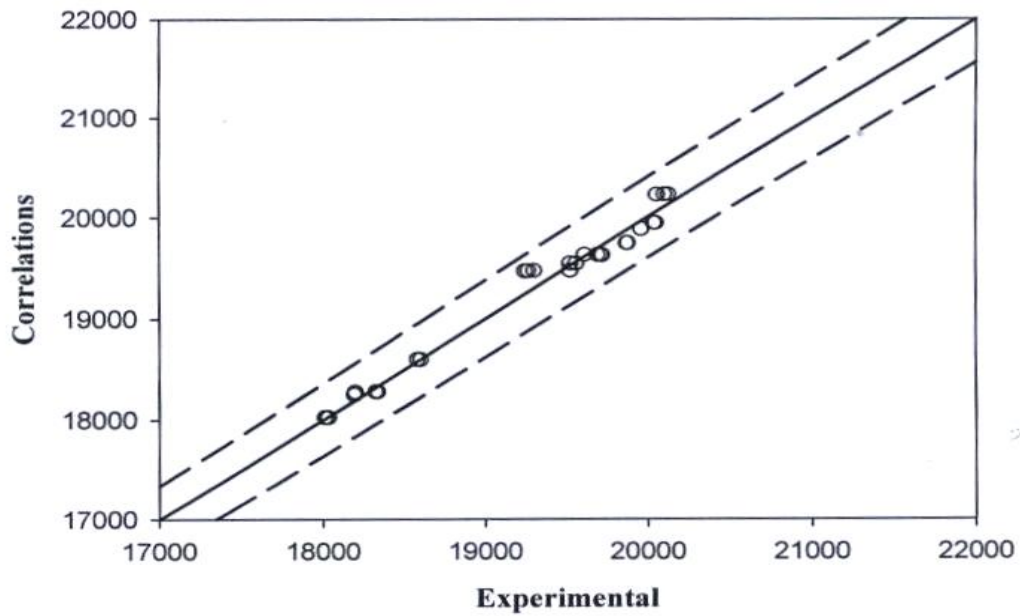


Figure (10): Comparison between experimental data and equation (5) and (6) for the pressure drop using tap water.

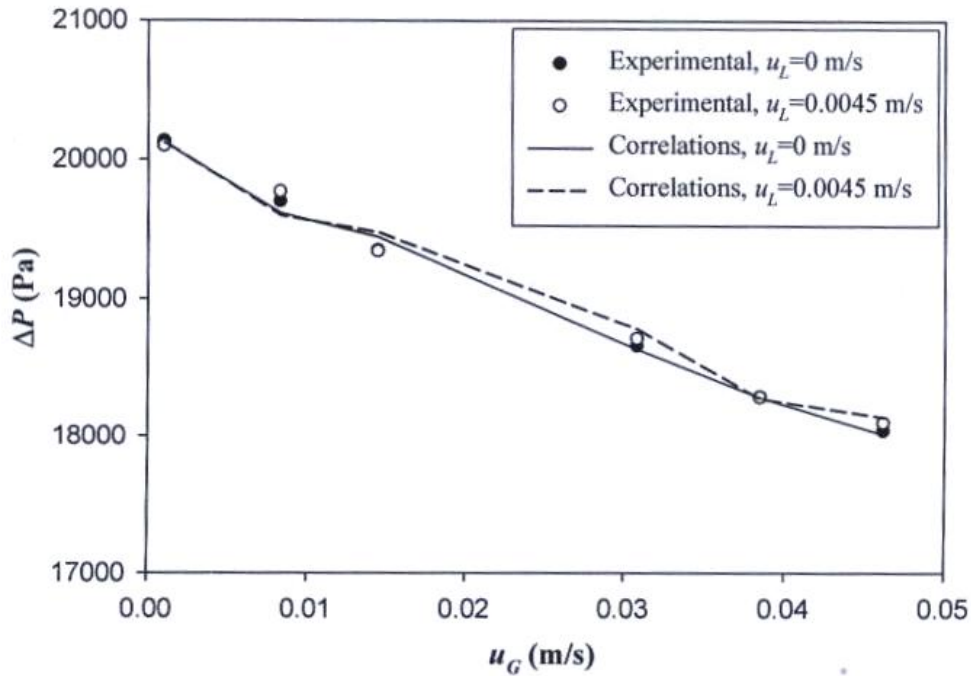


Figure (11) Pressure drop for 0.2% of CMC solutions.

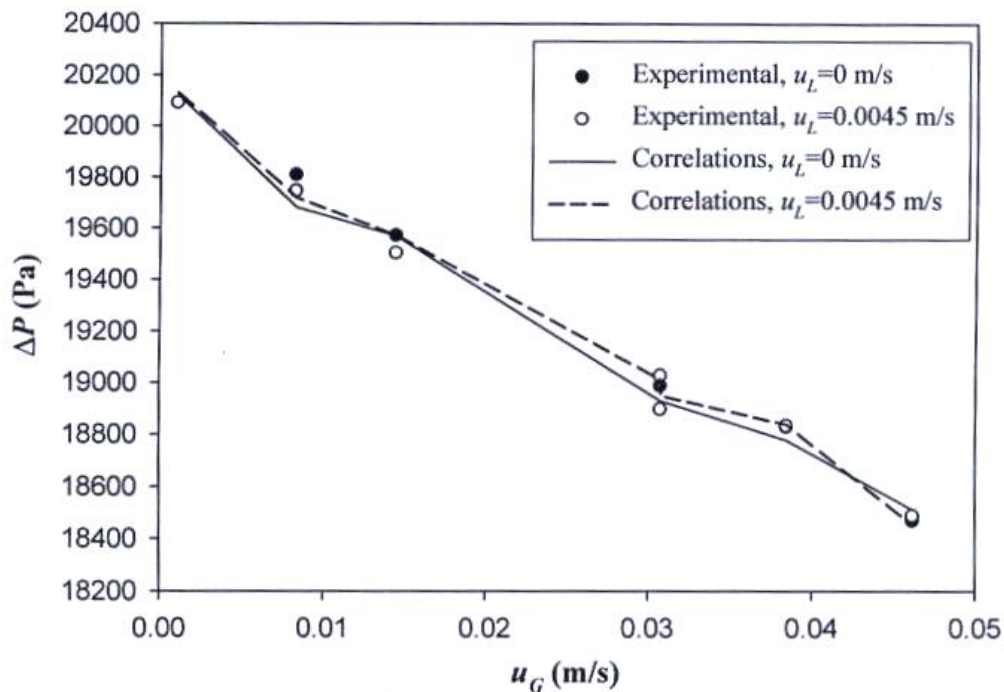


Figure (12) Pressure drop for 0.4% of CMC solutions.

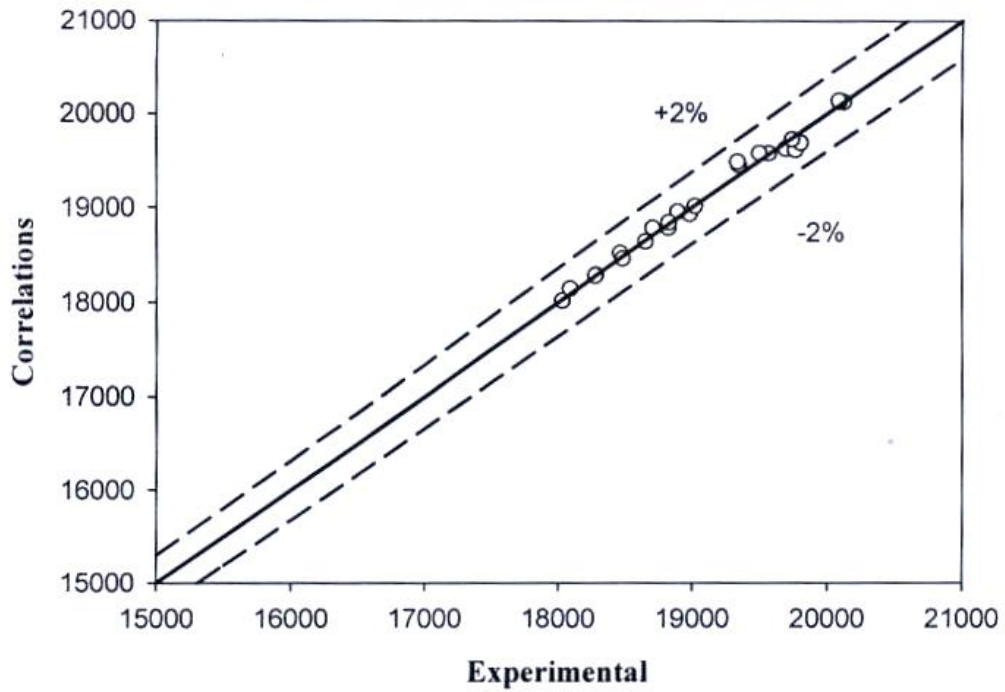


Figure (13): Comparison between experimental data and equation (7) and (8) for the pressure drop with CMC solutions